Microelectronic Engineering 147 (2015) 1–4

Contents lists available at ScienceDirect

Microelectronic Engineering

journal homepage: www.elsevier.com/locate/mee

Surface and interfacial study of half cycle atomic layer deposited Al_2O_3 on black phosphorus

Hui Zhu [a], Xiaoye Qin [a], Angelica Azcatl [a], Rafik Addou [a], Stephen McDonnell [a], Peide D. Ye [b], Robert M. Wallace [a,*]

[a] *Department of Materials Science and Engineering, 800 W. Campbell Road, RL10, University of Texas at Dallas, Richardson, TX 75080, USA*
[b] *School of Electrical and Computer Engineering and Birck Nanotechnology Center, Purdue University, West Lafayette, IN 47907, USA*

ARTICLE INFO

Article history:
Received 17 February 2015
Received in revised form 24 March 2015
Accepted 3 April 2015
Available online 8 April 2015

Keywords:
Black phosphorus
Black-P
ALD
Half-cycle
Phosphorene
2D semiconductors

ABSTRACT

The interfacial chemistry between the "half cycle" atomic layer deposited (ALD) Al_2O_3 and black phosphorus (black-P) was examined using *in situ* X-ray photoelectron spectroscopy (XPS). Two samples, native and freshly exfoliated, are investigated to understand the effect of oxidation on the initial ALD nucleation. It is found that annealing samples in the ALD chamber results in an increase of oxidation, caused most likely by oxygen transferring from surface adventitious contamination. After the half cycle ALD process, the P-oxide concentration increases, indicating interface deterioration during the Al_2O_3 deposition. Based on the Al_2O_3 nucleation or growth behavior observed in the half cycle ALD studies, a true ALD growth tends to occur only after formation of a complete monolayer of oxide on the clean black-P surface with minimum oxidation concentration.

© 2015 Elsevier B.V. All rights reserved.

1. Introduction

Black phosphorus, an anisotropic lamellar semiconductor, is considered an appealing two-dimensional (2D) material because of its novel properties and recent successful application in few-layer transistors [1,2]. Unlike graphene, bulk black-P displays a direct bandgap of about 0.3 eV [2–4], and an impressive hole mobility up to $10^4\,cm^2/(V\,s)$ at low temperatures [5], which is superior to transition metal dichalcogenides (TMDs) such as MoS_2. These properties indicate that black-P is a promising candidate for electronic and optoelectronic device applications. However, the strong hydrophilic [6,7] and photo-oxidative [4] properties of black-P raise important concerns regarding its chemical and physical stabilities during the device fabrication. Recent work by Wood et al. [8] and Castellanos-Gomez et al. [7] has shown that water droplets and oxidation can be detected on the surface of black-P after several hours of ambient exposure, and the surface is more severely oxidized if exposed for longer than 1 week, causing etching of some thin black-P flakes. This could be related to hydrogen (H) and hydroxyl (OH) adsorption which form strong bonds with P atoms and act as "chemical scissors" to break the P–P backbone bonds [9]. Thus, it is critical to develop an efficient isolation or passivation layer for the black-P surface to maintain intrinsic electronic properties for a longer time. Typical black-P based transistors use ALD of Al_2O_3 [2,6,10] or HfO_2 [11] as a dielectric layer for electrical isolation. Work by Luo et al. [6] specifically mentioned that a few-layer black-P metal oxide semiconductor field-effect transistor (MOSFET) with Al_2O_3 passivation can be ambient stable as long as 100 h. However, the detailed identification of the interfacial chemical states resulting from ALD Al_2O_3/black-P is unclear and important. In this study, *in situ* monochromatic XPS characterization of the interfacial chemistry was carried out to understand the evolution of interfacial interaction, chemistry and nucleation of Al_2O_3 after "half cycle" ALD Al_2O_3 on the native and the freshly exfoliated black-P surfaces, separately.

2. Materials and methods

The black-P samples used in this experiment were purchased from Smart Elements. One sample has native oxides ("native") present on the surface, while the other sample is mechanically exfoliated with Scotch® Magic™ Tape to remove layers.

To minimize ambient air exposure, the second sample was loaded into an ultrahigh vacuum (UHV) cluster system described elsewhere [12] after exfoliation within 5 min.

* Corresponding author. Tel.: +1 972 883 6638; fax: +1 972 883 5725.
E-mail address: rmwallace@utdallas.edu (R.M. Wallace).

http://dx.doi.org/10.1016/j.mee.2015.04.014
0167-9317/© 2015 Elsevier B.V. All rights reserved.

The *in situ* ALD depositions are performed in the UHV system, shown in Fig. 1, which integrates a Picosun 200R ALD chamber (base pressure ~4 mbar) through a turbo pumped load lock chamber (~1×10^{-7} mbar) [12]. *In situ* XPS is carried out in the analysis chamber. Thus, during the following half cycle ALD experiments, spurious contamination can be effectively avoided.

Fig. 2 shows the half cycle experiment procedure [13]. Trimethyl aluminum (TMA) and H_2O precursors were used for the Al_2O_3 deposition, with an argon (purity ~99.9997%, Airgas) carrier flow rate of 200 SCCM and a substrate temperature of 200 °C. Samples were transferred between the XPS analysis chamber and the ALD chamber under UHV to allow XPS scanning on the initial surfaces, after annealing to 200 °C, 1st pulse of TMA, 1st pulse of water, 2nd pulse of TMA, 2nd pulse of water, after the 5th, 10th, 20th, 30th, and the 40th full cycle (TMA + water). Here we use a monochromatic Al Kα X-ray source, which has a kinetic energy of 1486.7 eV, pass energy of 15 eV and a take-off angle of 45° relative to the sample normal. P 2*p*, Sn 3*d*, I 3*d*, C 1*s*, O 1*s* and Al 2*p* core level spectra were scanned and deconvoluted with AAnalyzer software [14].

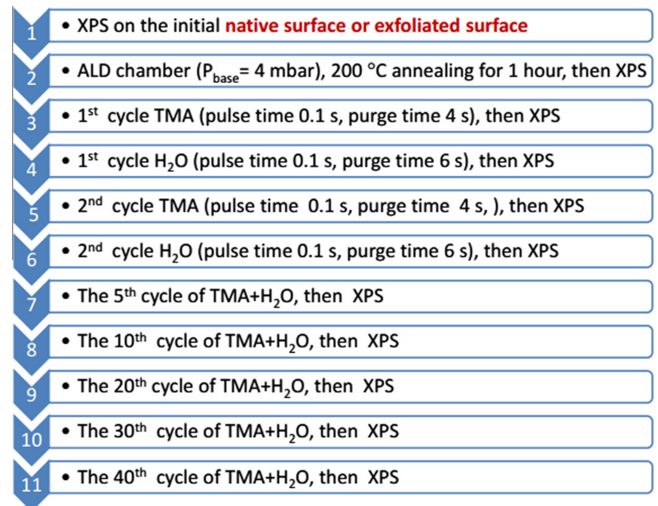

Fig. 2. The half cycle ALD deposition process of Al_2O_3 on black-P.

3. Results and discussion

A comparison of the normalized P 2*p* spectra of the native and exfoliated surfaces after 40 cycles of ALD is shown in Fig. 3. On the native surface, the native P-oxide peak detected at ~4.2 eV from the bulk black-P peak (P–P bonding) could be a combination of PO_x (i.e. P_2O_3) and P-OH chemical states because of their close binding energy ~134.2 eV. This peak is labeled as "PO_x". In comparison, the intensity of the PO_x peak from the exfoliated surface is lower than that detected from the native sample. The initial intensity ratio of the PO_x to bulk peak (PO_x/P–P) is ~10% on the native sample, and ~3% on the exfoliated sample. This suggests that the surface oxidation concentration on black P can be effectively reduced by removing the top a few layers with exfoliation. However, it can reform quickly even after exposure to ambient conditions for only a few minutes.

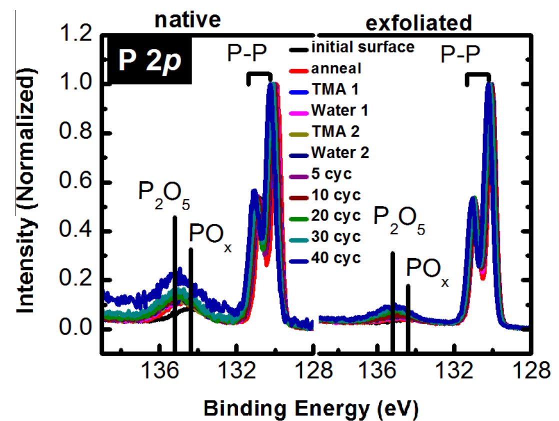

Fig. 3. A comparison of the P 2*p* core level XPS spectra from the native oxide and exfoliated samples during the ALD process.

After 200 °C annealing in the ALD chamber under Ar flow for 1 h, the P-oxide peak becomes broader, which is more apparently observed on the native oxide sample due to oxygen adsorption and saturation of P-oxide. With XPS deconvolution, we find that

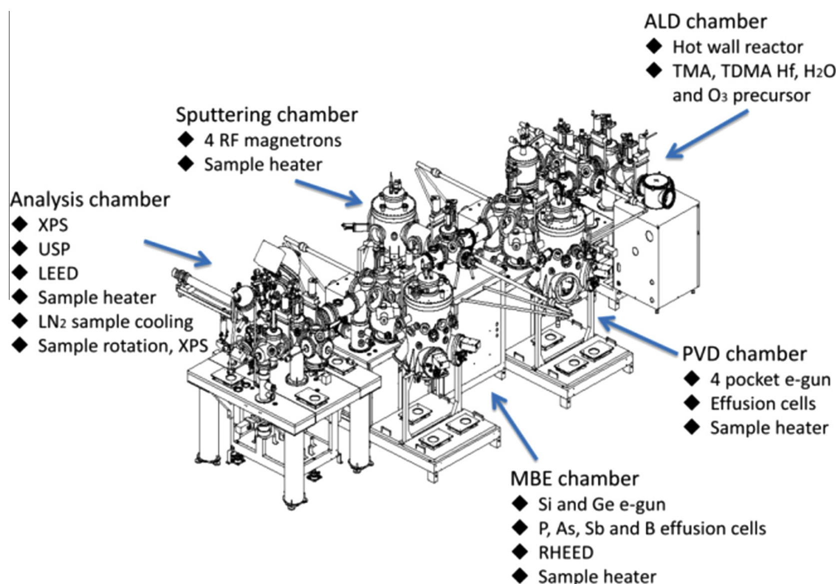

Fig. 1. The UHV cluster system.

a stable and oxygen saturated P-oxide state, P_2O_5, is generated. The P_2O_5 peak is shifted ~5.1 eV at a higher binding energy from the bulk P–P peak. At the same time, the ratio of the PO_x peak does not decrease. This clearly shows the stability of P-oxide at 200 °C and the generation of P_2O_5 is not only a phase transition of the PO_x state but also induced from chemical reaction with the surface adventitious oxygen contamination that is detected on both samples; otherwise the intensity of the PO_x peak would decrease.

Previous experimental results [15] suggested that P-oxide formed on black-P is unstable and tends to evaporate at 250 °C. In contrast, this is not observed in our experiments where the temperature did not exceed 200 °C. After annealing, the intensity ratio of the total P-oxide to the bulk black-P peak, $(PO_x + P_2O_5)$/P–P, increased to 19% and 5% on the native and the exfoliated sample, respectively.

The intensity ratio $(PO_x + P_2O_5)$/P–P during the half cycle process are calculated and presented in Fig. 4. The increasing ratio indicates that the oxidation continues on both samples during the ALD cycles. Recent DFT calculations [8] shows that water adsorption on the surface of black-P can only distort top most layers while the underlying crystal structure remains unchanged. Experimental results by Favron et al. [4] also indicate that exposing black-P to water under vacuum may not able to oxidize it. However, from the half cycle experiments, it appears that the H_2O precursor enhances the oxidation of black-P during the ALD process. We propose that the H_2O precursor reacts with the P-oxide or other defects, changing the surface reactivity of black-P and introducing more defects that facilitate reaction with surface oxygen, adventitious contamination, or H_2O precursors. Whether TMA or the H_2O precursor itself at 200 °C can damage the crystal surface of black-P or not still needs more direct evidence. In general, the total oxidation extent during the ALD process on these two samples is very similar: the intensity ratio $(PO_x + P_2O_5)$/P–P on both samples increases by ~10% after 40 cycles.

Fig. 5 shows the Al 2*p* spectra after 40 cycles of Al_2O_3 deposition. The higher intensity of the Al 2*p* peak from the native sample compared to the exfoliated sample, with a binding energy for Al 2*p* of ~75.8 eV, indicates the formation of a thicker Al_2O_3 on the native sample. This is also supported by the XPS thickness calculation, based on the attenuation of the integrated P 2*p* peak upon Al_2O_3 deposition. After 5 cycles, the thickness of Al_2O_3 is ~0.2 nm on the native surface while less than 0.1 nm on the exfoliated surface. Moreover, after 20 full cycles, there is ~0.5 nm and 0.2 nm of Al_2O_3 on the native and the exfoliated samples, respectively. This suggests that an initial nucleation period takes place before ideal ALD growth. The higher growth rate on the native sample is

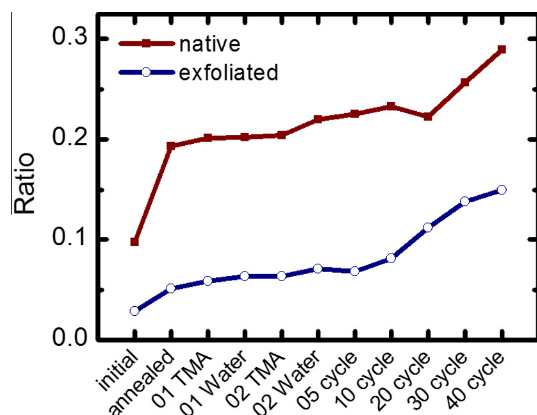

Fig. 4. The variation in the ratio of integrated intensity of the total P-oxide to that of the bulk black-P peak components, $(PO_x + P_2O_5)$/P–P, during the ALD process on the native and the exfoliated samples.

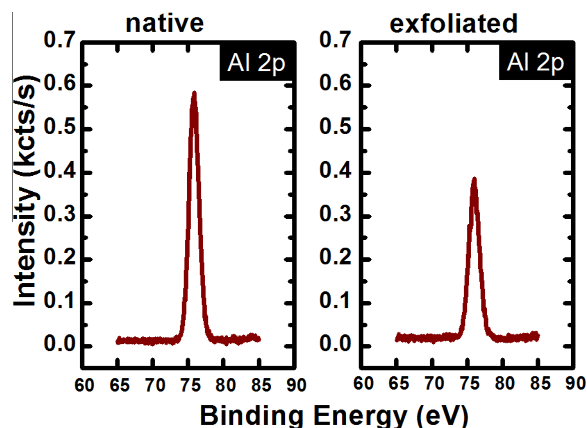

Fig. 5. Al 2*p* spectra after 40 cycles of Al_2O_3 deposition on the native and the exfoliated samples, respectively.

associated with a higher P-oxide concentration and probably a higher defect density on that surface as well. After 40 full cycles, the Al_2O_3 deposition thickness is ~2.47 nm on the native sample, and ~0.74 nm on the exfoliated sample.

4. Conclusion

In summary, we have studied the initial stages of ALD Al_2O_3 film growth on black-P using *in situ* XPS at each individual ALD "half cycle". Two samples were compared with one exhibiting a native oxide and the other slightly oxidized after exfoliation. After annealing in the ALD chamber at the Al_2O_3 deposition temperature (200 °C) for 1 h, the P-oxide concentration increases on the native sample surface as a result of the oxygen transfer from surface adventitious contamination. In addition, after successive ALD cycles, the Al_2O_3/black-P interface deteriorated by further oxidation. Previous research indicates that water exposure alone may not cause oxidation of black-P [4]. Therefore, the oxidation during the ALD process might be related to the original generated P-oxide which changes the surface reactivity or creates more defects. Moreover, with the increased P-oxide concentration on the native sample, which are likely preferred nucleation sites for the TMA precursor, results in the Al_2O_3 deposition thickness after 40 cycles is ~2.47 nm: much higher than that on the exfoliated sample (~0.74 nm). Finally, the Al_2O_3 growth on black-P requires a nucleation period before an ideal ALD growth.

Acknowledgments

This work is supported in part by the SWAN Center, a SRC center sponsored by the Nanoelectronics Research Initiative and NIST, the Center for Low Energy Systems Technology (LEAST), one of the six SRC STARnet Centers, sponsored by MARCO and DARPA, and the US/Ireland R&D Partnership (UNITE) under the NSF award ECCS-1407765.

References

[1] L. Li, Y. Yu, G.J. Ye, Q. Ge, X. Ou, H. Wu, D. Feng, X.H. Chen, Y. Zhang, Nat. Nanotechnol. 9 (2014) 372.
[2] H. Liu, A.T. Neal, Z. Zhu, Z. Luo, X. Xu, ACS Nano 8 (2014) 4033.
[3] Y. Harada, K. Murano, I. Shirotani, T. Takahashi, Y. Maruyama, Solid State Commun. 44 (1982) 877.
[4] A. Favron, E. Gaufrès, F. Fossard, P.L. Lévesque, Anne-Laurence, Phaneuf-L'Heureux, N.Y.-W. Tang, A. Loiseau, R. Leonelli, S. Francoeur, R. Martel, arXiv: 1408.0345 (2014).
[5] Y. Deng, Z. Lou, N.J. Conrad, L. Han, Y. Gong, S. Najmaei, P.M. Ajayan, J. Lou, X. Xu, P.D. Ye, ACS Nano 8 (2014) 8292.
[6] X. Luo, Y. Rahbarihagh, IEEE Electron Device Lett. 35 (2014) 2.

[7] A. Castellanos-Gomez, L. Vicarelli, E. Prada, J.O. Island, K.L. Narasimha-Acharya, S.I. Blanter, D.J. Groenendijk, M. Buscema, G.A. Steele, J.V. Alvarez, H.W. Zandbergen, J.J. Palacios, H.S.J. van der Zant, 2D Mater. 1 (2014) 025001.
[8] J.D. Wood, S.A. Wells, D. Jariwala, K. Chen, E. Cho, V.K. Sangwan, X. Liu, L.J. Lauhon, T.J. Marks, M.C. Hersam, Nano Lett. 14 (2014) 6964.
[9] X. Peng, Q. Wei, arXiv:1405.0801 1 (2014).
[10] H. Liu, A.T. Neal, M. Si, Y. Du, P.D. Ye, IEEE Electron Device Lett. 35 (2014) 795.
[11] N. Haratipour, M.C. Robbins, S.J. Koester, arXiv:1409.8395 2 (n.d.).
[12] R.M. Wallace, ECS Trans. 16 (5) (2008) 255.
[13] M. Milojevic, F.S. Aguirre-Tostado, C.L. Hinkle, H.C. Kim, E.M. Vogel, J. Kim, R.M. Wallace, Appl. Phys. Lett. 93 (2008) 202902.
[14] A. Herrera-Gómez, A. Hegedus, P.L. Meissner, Appl. Phys. Lett. 81 (2002) 1014.
[15] J. Brunner, M. Thuler, J. Phys. Chem. Solids 40 (1979) 967.